

## Fabricating Superhydrophobic Surfaces with Solid Freeform Fabrication Tools

Alan M. Lyons<sup>1,2\*</sup>, John Mullins<sup>2</sup>, Mark Barahman,<sup>1</sup> Itay Erlich,<sup>1</sup> and Todd Salamon<sup>3</sup>

<sup>1</sup>CUNY – College of Staten Island  
New York, NY, U.S.A.

<sup>2</sup>Bell Laboratories – Alcatel-Lucent  
Dublin, Ireland

<sup>3</sup>Bell Laboratories – Alcatel-Lucent  
Murray Hill, NJ U.S.A.

### *Abstract:*

Superhydrophobic surfaces exhibit a range of properties such as large contact angle, low contact angle hysteresis and decreased hydrodynamic drag. These properties make superhydrophobic surfaces of fundamental and commercial interest as they can enable a wide variety of applications including microfluidic components, biomedical devices, and micro-batteries. Superhydrophobic behavior is achieved through a combination of the hydrophobicity of the polymer and the roughness of the surface. We have used a commercially available multi-jet modeling rapid prototyping machine to fabricate 3D objects where the superhydrophobic surface is monolithic with the part. This approach was used to fabricate non-planar components with novel structures including helical conduits and porous meshes. In addition, we have developed a robotic dispensing tool that enables greater freedom of material selection. Both approaches have been used to fabricate arrays of surface features with diameters below 175 microns and with aspect ratios greater than 8:1. The fabrication and wetting properties of surfaces made using these two techniques will be discussed.

### **Introduction:**

Superhydrophobic surfaces are highly water repellent such that water droplets form a contact angle with the surface in excess of 150 degrees. This effect is due to a combination of the low solid surface free energy and extreme surface topography of the material. Drops of aqueous fluids are suspended on the tips of the structured surface elements and exhibit significant slip along the boundary. The fluid is primarily in contact with air; only a relatively small fraction (usually <5%) of the total fluid surface area is in contact with the solid surface. Drag reduction values of more than 50%, relative to a smooth surface, have been reported for flow in a water tunnel<sup>1</sup>. Reduction in flow resistance (drag) has been primarily observed for water. However, aqueous alcohol solutions have exhibited so-called superlyophobic behavior for static droplets<sup>2</sup>.

Such surfaces occur naturally in both plants<sup>3</sup> as well as animals<sup>4</sup> and the fabrication and properties of synthetic superhydrophobic surfaces have been reported by numerous authors<sup>5</sup>. In most of these studies, the synthetic surface is fabricated by the photolithographic definition of

---

\* Corresponding author

silicon wafers to create arrays of silicon posts with diameters ranging from 100nm<sup>6</sup> to 100um<sup>7</sup>. Using photolithography to create superhydrophobic surfaces enables a wide variety of surface patterns to be formed with a high degree of precision.

Despite the control afforded by photolithography, there are several limitations imposed by this process for the fabrication of useful, low-cost superhydrophobic components. Cost is one issue. Silicon wafer processing is expensive, especially considering the cost of tools and the time required to etch high aspect ratio, fine-pitch posts deep into the surface. Reliability of the surfaces is a second important factor. The silicon surface rapidly oxidizes to form SiO<sub>2</sub> which is hydrophilic. Thus the nano/micro textured silicon surfaces must be treated with a coating to render the surface hydrophobic. Coatings include fluoro-silanes, fluoropolymers and plasma deposited fluorocarbon films. Such coatings on silicon have been found to exhibit adhesion loss with long term exposure to water<sup>8</sup> causing the surface to lose its superhydrophobic properties. Finally, and perhaps most significantly, photolithography is inherently a planar process. The surface must be flat to insure the image remains in focus and maintain linewidth control. However, it is extremely challenging to fabricate channels and other complex, inherently three-dimensional surface shapes with a planar lithography approach.

In this paper, we describe the use of solid freeform fabrication (SFF) technologies to fabricate superhydrophobic surfaces and 3D structures from hydrophobic polymers<sup>9</sup>. The SFF approach address the three limitations imposed by lithographic processes as the SFF technologies are robust and offer a relatively low-cost route to fabricating superhydrophobic components. As the polymers used to fabricate the superhydrophobic structures are themselves hydrophobic, coatings are not required and adhesion issues are eliminated, rendering structures which are more reliable. Finally, three-dimensional parts, such as conduits, helices and membranes<sup>10</sup> can be fabricated with commercial machines and readily available CAD modeling software.

Ordered arrays of micro-textured features (>150 micron diameter) were built into arbitrarily shaped three-dimensional structure including tubes and helices by using a commercially available polymer-jetting technique. The superhydrophobic properties, such as roll-off angle and water head pressure, were demonstrated to be governed by the same equations as for micro- and nano-scale superhydrophobic surfaces patterned on silicon. In addition, we used a robotic dispensing system to build surfaces with silicone polymers which are not compatible with commercially available SFF systems.

### **Experimental:**

Commercial 3D Printer: An InVision-HR 3-D printer from 3D Systems was used to fabricate parts. This machine uses multi-jet modeling technology combined with a UV-curable urethane-acrylic model material (VisiJet HR200) and a wax-based support material (VisiJet S100). After the build, the support material was removed in a forced-air convection oven at 70°C. Parts were designed using ProEngineer or 3dsMax software and exported as STL files to the InVision-HR.

Robotic Dispenser: A robot (Janome-2203N) with +/- 10 micron repeatability was used as an XYZ platform and trigger for a syringe controller (EFD Performus) and a UV lamp (Dymax BluWave 200) as shown schematically in Figure 1. Two different materials were used

for building the posts: A viscous room temperature vulcanizing (RTV) silicone (DAP aquarium sealant) and a UV curable silicone (Dymax Cure-Point 9440 AB-Mix). To control the rheological properties of the low viscosity 9440, 10 parts per hundred of fumed silica (Cab-o-Sil TS 530) was dispersed into the adhesive to provide thixotropy. The materials were carefully loaded into 10cc polyethylene syringe barrels, avoiding air bubble entrapment, and capped with either a 27 gauge (210  $\mu\text{m}$  i.d.) tapered tip with the RTV, or a 33 gauge (100 $\mu\text{m}$  i.d.) chamfered steel tip with the UV curable adhesive. Both the syringe and UV light-guide were mounted parallel to each other on the robotic arm such that the adhesive drop was exposed to UV light only after the arm was translated by 18.5 mm after the dispense step was complete. Glass microscope slides were used as substrates and placed on top of an aluminum stage. The dispense cycle program repeated the following sequence to create an array of posts:

- bring the arm to a predetermined dispense height above a substrate
- trigger the syringe controller to dispense at a pre-set time and pressure
- lift the syringe normal to the surface
- *For single dispense posts:* translate the syringe to the next dispense location or
- *For multi-layer posts:* translate the arm to position the UV light guide above the dispense location, trigger the UV lamp for a pre-set time and translate to the next dispense location.

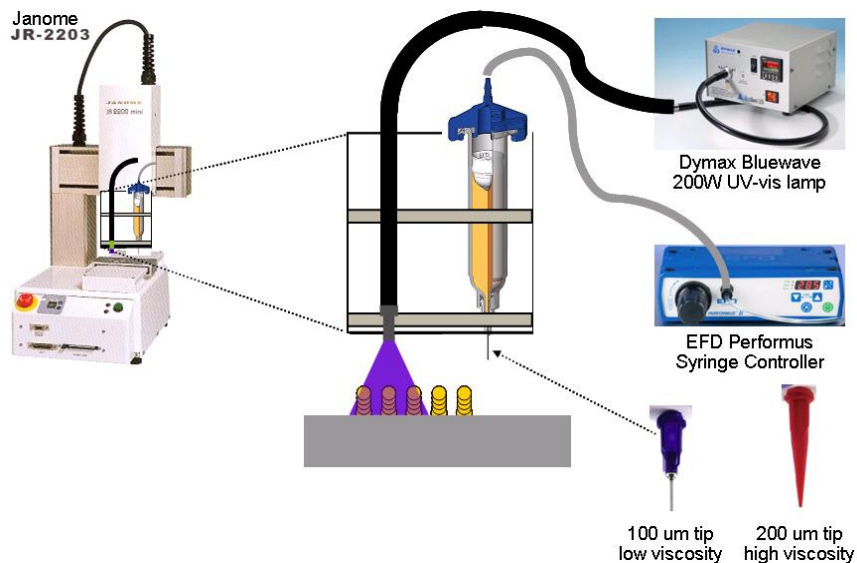


**Figure 1: Schematic of the robotic dispensing system with UV lamp**

Experimental Measurements: The height of a water column supported by a superhydrophobic sample was measured on samples covered with a 25mm x 25mm array of posts and fitting a square tube of the same material above the sample. Water was added slowly to the chamber created by the tube and the sample base until the transformation from Cassie (non-wetted) to Wenzel (fully-wetted) state was observed visually. This transition was easily and reproducibly observed due to the change in refractive index between air and polymer. Contact angles were measured using a ramé-hart model 250 goniometer.

## Results and Discussion:

Commercial 3D Printer: Parts made with the InVision-HR machine exhibited good image fidelity and measured part dimensions agreed well with CAD specifications. Arrays of cylindrical (Figure 2a), square and square-based pyramidal posts (Figure 3) were successfully created. Droplets of water placed on these post arrays exhibited superhydrophobic behavior as shown in Figure 2b.

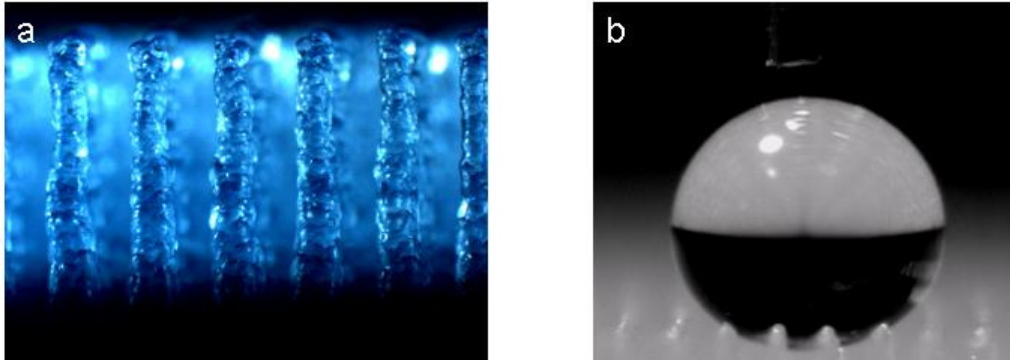


**Figure 2:** (a) Cylindrical posts fabricated using a InVision 3-D printer measuring 175 micron diameter x 1300 microns tall; and (b) a 2mm diameter water droplet posed atop a similar surface demonstrating superhydrophobic behavior.

Post arrays faithfully replicate the pitch and build height specified by the CAD model as illustrated for the case of square-based pyramidal shaped posts over the range from 300 to 500 micron pitch in Figure 3. Each square-based pyramidal post is designed to have a 200 x 200 micron base with a height of 1000 microns. At 250 micron pitch, however, the posts overlap at the base reducing the relative post height by almost 40% from the nominal value of 1000 microns.

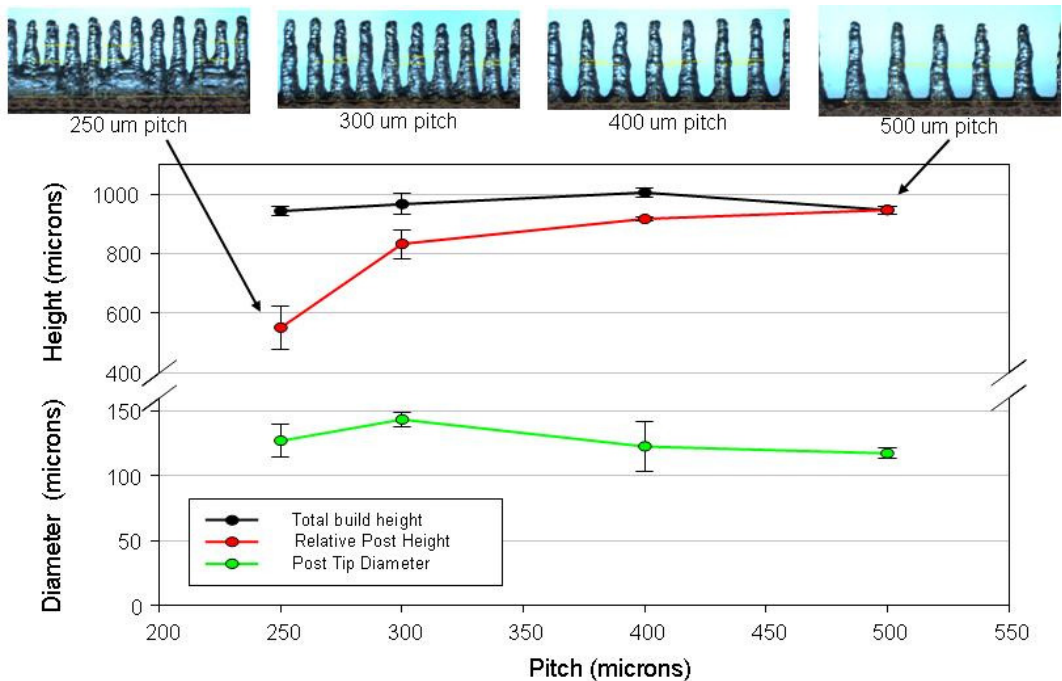


**Figure 3:** Effect of post pitch on height and diameter of square-based pyramidal posts

Arrays of posts were integrated into the surface of more complex structures in CAD models and successfully printed as monolithic objects. Tubes, conduits and helices were fabricated, either as building blocks (Fig 4a) which could be assembled into any arbitrary pathway (Fig 4b) or as contiguous objects, limited in size only by the constraints of the printing equipment (Figure 4c). Conical helix pathways, such as the one shown in Figure 4c, were fabricated both with and without arrays of posts integrated into the conduit surface. When no surface features were present, water droplets experienced sufficient drag that they remained stationary until a sufficient number of droplets coalesced such that the mass of water exceeded a threshold value allowing a large drop of water to slide partway down the path. When the conical helix conduit surface was formed with arrays of posts, however, water droplets rolled readily along the conduit due to the low drag at the water-surface interface. Releasing water droplets at a fixed frequency from a syringe formed a periodic stream of individual droplets with the same frequency.

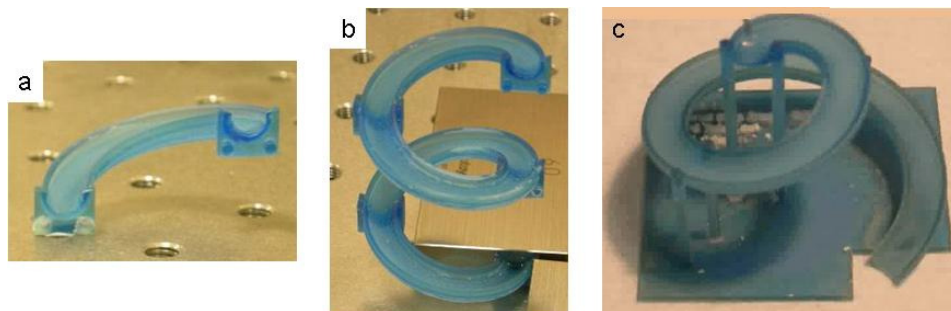


**Figure 4 Superhydrophobic helical building block with connectors at each end (a) Four helical units assembled into a two-turn helix (b) A monolithic conical helix measuring 75mm x 75mm x 50mm tall (c).**

The behavior of water on superhydrophobic surfaces fabricated by 3D printing are governed by the same equations as those for superhydrophobic surfaces fabricated with nano-scale features<sup>11</sup>, which are based on a balance of surface tension and hydrostatic forces. This is illustrated in Figure 5 for the case of the fluid pressure that such structures can support. For water supported on round-headed posts, the fluid height can be calculated<sup>11</sup>:

$$h = \frac{\gamma \pi D \sin(\theta - \pi/2)}{\rho g L^2 - \frac{\pi}{4} D^2}$$

where  $\gamma$  is the surface tension,  $\rho$  is the density of the fluid,  $g$  is gravitational acceleration,  $D$  is the diameter of the post heads,  $L$  is the space between posts and  $\theta$  is the advancing contact angle ( $113^\circ$  for the HR200 model material). This relationship is plotted as the green curve using the diameter values shown in Figure 3. This plot has a similar shape to the experimental measured values (blue curve Fig 5, but diverges as the pitch decreases. This may result from the water

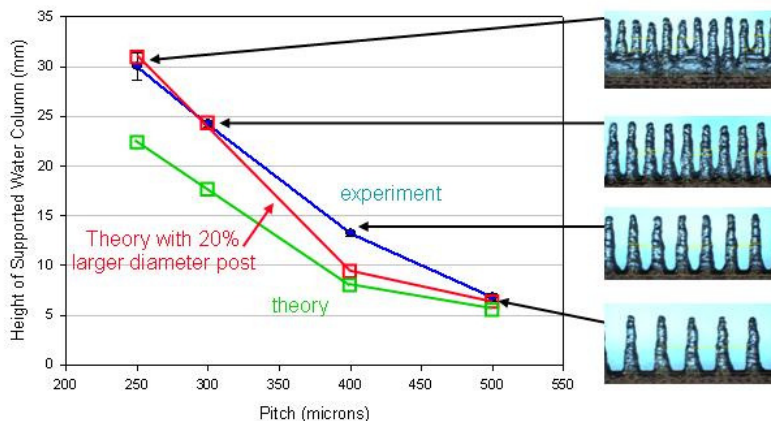


**Figure 5: Effect of post pitch on the height of water that can be supported**

droplet penetrating partially into the post tips as has been observed for posts with  $<200\text{nm}$  diameter<sup>11</sup>. Optimizing the fit of the theoretical curve to the experimental values requires increasing the post diameter by 20% (red curve in Fig 5). This would require the droplet descending approximately 130 microns into the posts, which is reasonable given their taper.

The base for these experiments serves mainly to support the post arrays. However, since the droplet is suspended on (or near) the post tips, the base could equally well be made from a porous mesh, so long as the post pitch can be maintained. Porous superhydrophobic conduits have been constructed, as shown in Figure 6, such that aqueous fluids are supported while

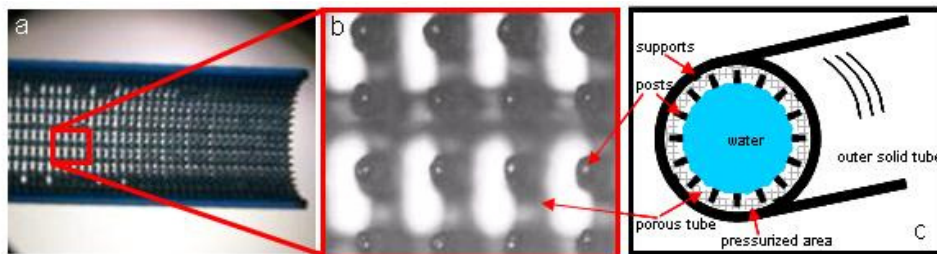


**Figure 6: (a) Porous superhydrophobic conduit 10mm in diameter(a); (b) Detailed view of (a) with posts measuring 150  $\mu\text{m}$  diameter x 1500  $\mu\text{m}$  tall; and (c) Schematic cross-section of pressurized superhydrophobic tube.**

permitting an unrestricted flow of gas through the tube. In this way the droplet can interact with the gaseous atmosphere unrestricted by diffusion through a solid support base. By inserting this porous superhydrophobic tube inside a solid tube, the region between the solid and porous tubes may be pressurized with a gas. The gas pressure could be adjusted to maintain the liquid/gas interfacial pressure differential to within the value supported by the superhydrophobic micro-textured features.

Robotic Dispensing System. The commercially available multi-jet printer easily fabricated a variety of superhydrophobic parts. However this printer has certain limitations including material selection and resolution. To expand the range of materials that could be used to form superhydrophobic surfaces, we developed a robotic dispensing system with a UV lamp and light guide to enable in-situ curing of photosensitive materials. By modifying the tip

diameter, dispense pressure and dispense time, both a high viscosity RTV silicone as well as a low viscosity UV curable adhesive were dispensed.

**RTV Silicone:** Superhydrophobic surfaces were fabricated from arrays of RTV posts with pitches ranging from 450 to 700 microns. A single drop was used to fabricate each post. A ~5uL drop of water on a 500 pitch RTV post array is shown in Figure 7, which has an apparent contact angle >170 degrees. In contrast, the contact angle of water on a flat silicone sample is 110°. The tilt angle required for a water droplet to roll off a RTV silicone superhydrophobic surface is 20° for volumes between 10-20 uL. Droplets 8 uL and smaller required significantly higher angles (> 28°) as the diameter of the droplet becomes comparable to the pitch of the posts.

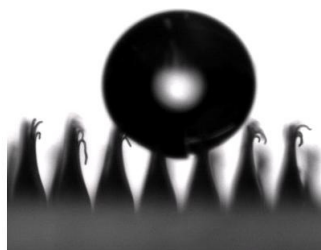


**Figure 7: Water droplet on an RTV silicon superhydrophobic surface with 500 um pitch posts**

The shape of the post was dependent upon several factors including the syringe position relative to the substrate during dispensing (dispense height) as well as the direction of the syringe tip motion after dispensing was completed. Reducing the pitch further causes the bases of the posts to overlap whereas increasing the pitch above 700 pitch allows the water droplet to penetrate the post surface and wet the side walls and base.

The effect of dispense height on post shape can be seen in Figure 8. When the syringe tip is close to the substrate, the RTV is forced to flow laterally, increasing the diameter of the post base (Fig 8a). As the dispense height increases, lateral flow decreases, reducing the post base diameter and forming a post that has a more uniform diameter along its height (fig 8d). If the dispense height becomes too large the drop does not reproducibly touch the substrate resulting in missing posts. The optimal dispense height for uniform posts for a superhydrophobic surface is between 250um-500um.

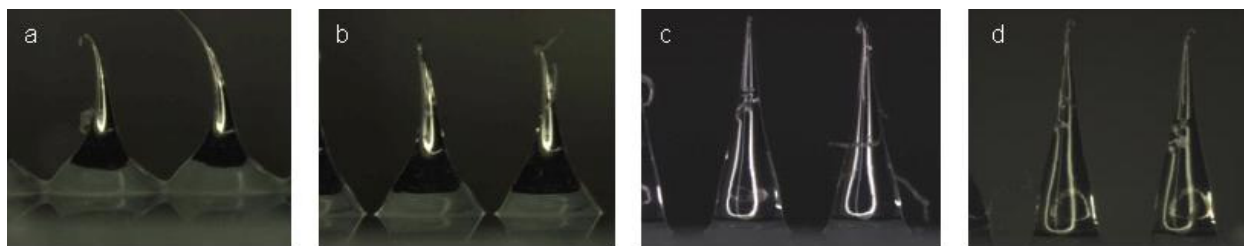


**Figure 8: RTV silicon posts fabricated by dispensing through a 27 gauge tapered tip at height of: (a) 100 um; (b) 190 um; (c) 250 um; and (d) 300 um above a glass substrate.**

The shape of the posts can be controlled by adjusting the direction of the dispensing tip motion after the dispense cycle is completed. For the posts in Figure 8, the tip was moved upwards, normal to the surface until the material disengaged from the tip. Angled posts were

intentionally made through a two step release process. Immediately after dispensing, the robot arm moved upwards 800 microns (normal to the surface), at which point the dispensed adhesive was still attached to the tip. The arm then rises at a 63° angle during which time the adhesive detaches from the tip forming an asymmetric post in the direction of the tip motion as shown in Figure 9.

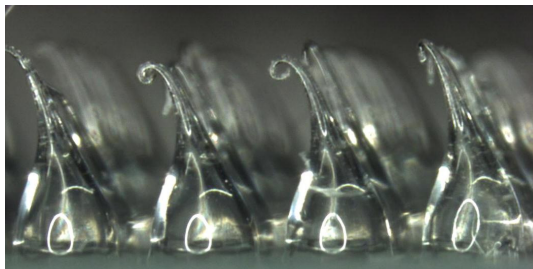


**Figure 9:** Tilted RTV posts created by raising the dispenser at a 63° angle during release.

These surfaces display a direction dependent roll off angle, where the roll off angle in the direction of the tilt is about 10° less than the roll off angle in the opposite direction.

**UV Curable Silicone:** Superhydrophobic surfaces with pitches of 350,400,450 and 500 microns have been made by dispensing multiple layers of individual drops of the adhesive and curing after each dispense. Modifying the rheology of the Dymax adhesive was essential for controlling the diameter and height of the posts. The viscosity of the as-received material was 1000 cps; dispensing this material would result in rapid flow across the substrate. By adding fumed silica, the low viscosity adhesive became thixotropic and so exhibited little flow before curing. With this rheology, further reduction in pitch should be possible, but would require the use of smaller diameter dispensing tips. The contact angle of water on a flat surface prepared from the Dymax UV curable silicone formulated with the thixotropic agent is 115°. This value is dramatically increased on a surface containing posts made of this material. Observed contact angles between this type of surface and a 5uL drop range between 157° and 169°.

Similar to fabricating RTV posts, the height of the dispense tip above the previously deposited layer has a significant effect on the overall shape of the resulting post. When the syringe tip is programmed to increment a relatively small amount between layers, the post spreads laterally causing the diameter of the post to increase as it rises above the surface (Fig 10a). Uniform post diameters were achieved by maintaining the correct dispense height for each layer as shown in Figure 10b.

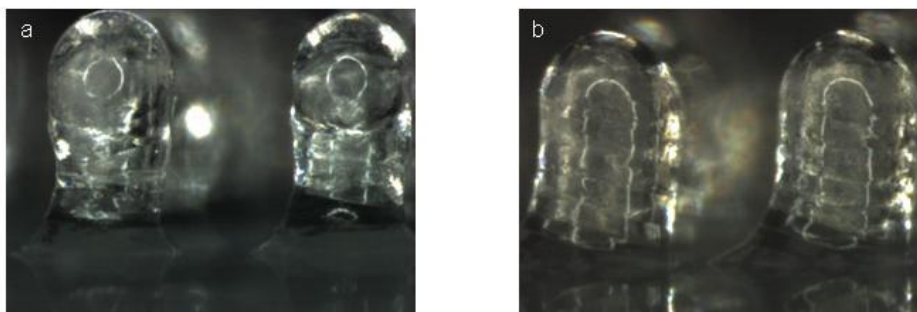


**Figure 10:** Effect of layer dispense height on the shape of UV cured silicone posts.

Post diameter is strongly affected by the dispense duration as shown by the red curve in Figure 11. Shorter dispense times resulted in smaller post diameters, approaching the inside diameter of the tip. The diameter measured at the base of the post is larger than the overall post diameter due to wetting characteristics between uncured adhesive and glass substrate. For a dispense time of 200ms, the base spreading is 155% of the post diameter, while at 70ms it is minimized to be 100% (or equal to) the post diameter. Decreasing dispense time significantly reduces the flow of excess material down the post as shown by the clearly delineated layers in Figure 12.

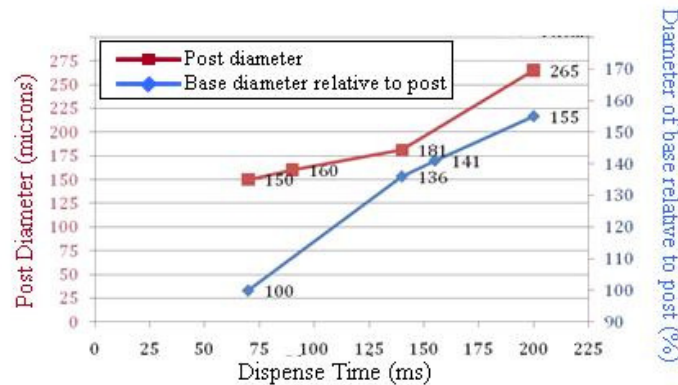


**Figure 11: Effect of dispense time in milliseconds on average post diameter in microns (red) and base spreading shown as the percent increase in diameter measured at the base relative to the post diameter (blue).**



**Figure 12: UV cured silicone posts at 400 um pitch fabricated by dispensing 23 layers of adhesive. Posts measure 175 um in diameter and 800 um tall.**

Another parameter that affects post diameter, spreading and shape is the UV dose. Curing with UV hardens the silicone preventing flow and allowing for effective layer stacking. A dose of  $100 \text{ J/cm}^2$  was required to produce the 23 layer stack in Figure 12. An insufficient dose resulted in short cone-shaped posts whereas additional cure times had no subsequent effect.

**Conclusions:** Superhydrophobic surfaces were prepared on a wide variety of surface shapes using a commercially available 3D printer. Fabrication of large, complex polymer objects including conduits, helices and conical helix structures was achieved where the micro-textured surface is monolithic with the body. The superhydrophobic behavior, such as the water column height supported, is easily measured and can be described by the same equations as those used to describe superhydrophobic behavior on surfaces with nano-scale textural features. By eliminating the need for hydrophobic coatings, these structures are expected to exhibit reliable superhydrophobic behavior.

To expand upon the limited material set available with commercially available printers, a dispensing robot system was developed which accommodates a wide selection of materials with different rheological properties and cure requirements (room temperature & UV cured). Arrays of posts were formed either from the deposition of single droplets (high viscosity materials) or the build-up of multiple thin layers (thixotropic materials). In both cases, good control of post shape and feature dimensions were achieved. We anticipate that this approach will enable the fabrication of superhydrophobic components that will be useful for a variety of applications in the biological and separation science areas.

### **Acknowledgements:**

This work was supported by IDA Ireland and NYSTAR, the New York State Foundation for Science, Technology and Innovation.

### **References**

---

<sup>1</sup> Henoeh, C.; Krupenkin, T.N.; Kolodner, P.; Taylor, J.A.; Hodes, M.S.; Lyons, A.M.; Peguero, C.; Breuer, K.S. Turbulent Drag Reduction Using Superhydrophobic Surfaces. *3rd AIAA Flow Control Conference*, San Francisco, CA, June 5 – 8, **2006**, 3192.

<sup>2</sup> Ahuja, A.; Taylor, J.A.; Lifton, V.; Sidorenko, A.A.; Salamon, T.R.; Lobaton, E.J.; Kolodner, P.; Krupenkin, T.N. Nanonails: A Simple Geometrical Approach to Electrically Tunable Superhydrophobic Surfaces. *Langmuir* **2008**, *24*, 9-14.

<sup>3</sup> Neinhuis, C.; Barthlott, W. Characterization and Distribution of Water-repellent, Self-cleaning Plant Surfaces. *Annals of Botany* **1997**, *79*, 667-677.

<sup>4</sup> Gao, X; Jiang, L. Water-repellent Legs of Water Striders, *Nature* **2004**, *432*, 36.

<sup>5</sup> Callies, M.; Quere, D. On water repellency. *Soft Matter* **2005**, *1*, pp 55–61.

<sup>6</sup> Krupenkin, T.N.; Taylor, J.A.; Schneider, T.M.; Yang, S. From Rolling Ball to Complete Wetting: The Dynamic Tuning of Liquids on Nanostructured Surfaces, *Langmuir* **2004**, *20*, 3824-3827.

<sup>7</sup> Oner, D.; McCarthy, T.J. Ultrahydrophobic Surfaces. Effects of Topography Length Scales on Wettability, *Langmuir* **2000**, *16*, 7777-7782.

<sup>8</sup> Gnanappa, A.K.; Slattery, O.; Peters, F.; O'Murchu, C.; O'Mathuna, C.; Fahey, R.; Taylor, J.A.; Krupenkin, T.N. Factors influencing adhesion of fluorocarbon (FC) thin film on a silicon substrate, *Thin Solid Films* **2008**, *516*, 5673–5680.

<sup>9</sup> Kempers, R.S.; Lyons, A.M.; O'Loughlin, A. Superhydrophobic Surfaces and Fabrication Process. U.S. Patent Application, 20070259156, **2007**.

<sup>10</sup> Lyons, A.M.; Mullins, J.; Schabel, M.J. Fluid-Permeable Body Having a Superhydrophobic Surface. U.S. Patent Application, 20080131653, **2008**.

<sup>11</sup> Lobaton, E. J.; Salamon, T. R. Computation of Constant Mean Curvature Surfaces – Application to the gas-liquid interface of a pressurized fluid on a superhydrophobic surface, *J. Colloid and Interface Science*, Volume 314, Issue 1, **2007**, Pages 184-198.